1440 *Inorg. Chem.* **1994,** *33,* 1440–1447

Preparation, Structures, and Fluxional Behavior of Organolithium Derivatives of a 1,5-Diphosphadithiatetrazocine and Their Complexes with Platinum(II) and Palladium(II)

Tristram Chivers,* Mark Edwards, Robert W. Hilts, Masood Parvez, and Rainer Vollmerhaus

Department of Chemistry, The University of Calgary, Calgary, Alberta, Canada T2N 1N4

Received December 29, 1992[⊗]

The reaction of the diphosphadithiatetrazocine 1,5-$Ph_4P_2N_4S_2$ with organolithium reagents RLi (R = Me, Bu^t, Ph, CH_2PPh_2) in THF generates Li[$Ph_4P_2N_4S_2R$]. An X-ray structural determination shows that the phenyl derivative is a dimer [Li($Ph_4P_2N_4S_2Ph$)·THF]$_2$ with a step-shaped structure. The phenyl group is attached to sulfur, and each lithium atom is coordinated, almost symmetrically, to two nitrogen atoms on the opposite side of the $P_2N_4S_2$ ring and to one nitrogen atom of the other $P_2N_4S_2$ ring. A single THF molecule completes the coordination sphere of the lithium atoms. The crystals of [Li($Ph_4P_2N_4S_2Ph$)·THF]$_2$ are triclinic, space group $P\bar{1}$, with a = 13.189(10) Å, b = 13.355(8) Å, c = 11.760(5) Å, α = 90.67(4)°, β = 114.15(4)°, γ = 114.05(5)°, V = 1683(2) Å^3, and Z = 2. The final R and R_w values were 0.072 and 0.060, respectively. ^{7}Li and ^{31}P NMR investigations of [Li($Ph_4P_2N_4S_2R$)·THF]$_2$ (R = Me, Bu^t, Ph, CH_2PPh_2), as a function of temperature and concentration in THF, show that these dimers are fluxional and provide evidence for a second species, which is tentatively identified as a symmetrical dimer with two molecules of THF coordinated to each lithium atom. The treatment of Li[$Ph_4P_2N_4S_2Me$] with iodomethane gives the *S,S'*-dimethyl derivative 1,5-$Ph_4P_2N_4S_2Me_2$ and the reaction of Li[$Ph_4P_2N_4S_2R$] with $MCl_2(PEt_3)_2$ (M = Pt, Pd) produces metal complexes of the type *trans*-$MCl(PEt_3)_2(Ph_4P_2N_4S_2R)$ (M = Pt, R = Me, Bu^t, Ph, CH_2PPh_2; M = Pd, R = Me) in which the metal and the R group are attached to opposite sulfur atoms. A variable-temperature ^{31}P NMR study of these metal complexes reveals an intramolecular dynamic exchange of the inequivalent PEt_3 groups, which is attributed to rotation about the metal–sulfur bond. The activation energy for this exchange is *ca.* 45 kJ mol^{-1} and is essentially independent of the nature of the R group attached to the other sulfur atom or the identity of the metal. The reaction of Li[$Ph_4P_2N_4S_2Me$] with *cis*-$PtCl_2(PPh_3)_2$ in THF at 65 °C produces $Pt(PPh_3)_2(\eta^2\text{-}Ph_4P_2N_4S_2\text{-}S,S')$ and $Pt(PPh_3)(\eta^1\text{-THF-}O)(Ph_4P_2N_4S_2)$ in an approximately 2:3 molar ratio.

Introduction

An intriguing feature of the chemistry of the unusual cage molecule S_4N_4 is the formation of ring-contracted products upon reaction with nucleophilic reagents.[1] For example, the reactions of S_4N_4 with anionic nucleophiles,[2] including organolithium reagents,[3] produce the six-membered ring $S_3N_3^-$. 1,5-Diphosphadithiatetrazocines **1** share a common structural feature with S_4N_4, i.e. a weak transannular S–S bond [d(S–S) = 2.5–2.6 Å].[4] These inorganic heterocycles act as good models for reactions of S_4N_4 that occur at the sulfur centers with the added advantages that the NPN units serve as a convenient NMR probe and help to maintain the structural integrity of the eight-membered ring. Thus the oxidative-addition of halogens to **1a** produces 1,5-$Ph_4P_2N_4S_2X_2$ (X = Cl, Br)[5] while the reactions of **1a–c** with platinum(0) or palladium(0) reagents yields the η^2-S,S'-bonded complexes $M(PPh_3)_2(R_4P_2N_4S_2)$ (M = Pt, Pd; R = Ph, Me, Et).[6]

The purpose of this study was to characterize the initial products of the reactions of **1** with anionic nucleophiles and to explore the synthetic potential of the anions so formed. To this end we have examined the products of the reactions of **1** with the organolithium reagents RLi (R = Me, Bu^t, Ph, CH_2PPh_2). The solid state structure of one of the products of these reactions, *viz.* [Li($Ph_4P_2N_4S_2Ph$)·THF]$_2$ was determined by X-ray crystallography, and the solution structures of the entire series [Li($Ph_4P_2N_4S_2R$)]$_2$ (R = Me, Bu^t, Ph, CH_2PPh_2) were investigated as a function of temperature and concentration by ^{7}Li and ^{31}P NMR spectroscopy.[7] The reactions of [Li($Ph_4P_2N_4S_2R$)]$_2$ with sources of electrophiles such as iodomethane and *cis*- or *trans*-$MCl_2(PR_3)_2$ (M = Pd, R = Et; M = Pt, R = Et, Ph) were also investigated. The structures of the metal complexes obtained in this way were determined by variable-temperature ^{31}P NMR spectroscopy and, in one case, by X-ray crystallography.[8]

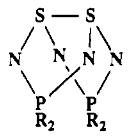

1a, R = Ph
1b, R = Me
1c, R = Et

Experimental Section

Reagents and General Procedures. All manipulations were carried out under dry nitrogen gas or argon in Schlenk vessels using standard air-sensitive techniques. Sodium benzophenone ketyl was used as a drying agent for all solvents, except dichloromethane, which was distilled over P_4O_{10}. The compounds 1,5-$R_4P_2N_4S_2$ (R = Ph, Me, Et),[4] *cis*-$PtCl_2(PEt_3)_2$,[9] *cis*-$PtCl_2(PPh_3)_2$,[10] *trans*-$PdCl_2(PEt_3)_2$,[11] and [$Ph_4P_2N_4S_2Me$]-

---

[⊗] Abstract published in *Advance ACS Abstracts,* February 15, 1994.

(1) Chivers, T.; Oakley, R. T. *Top. Curr. Chem.* **1982,** *102,* 117.

(2) Bojes, J.; Chivers, T.; Drummond, I.; MacLean, G. *Inorg. Chem.* **1978,** *17,* 3668.

(3) Jones, R.; Kelly, P. F.; Williams, D. J.; Woollins, J. D. *Polyhedron* **1987,** *6,* 1541.

(4) (a) Burford, N.; Chivers, T.; Codding, P. W.; Oakley, R. T. *Inorg. Chem.* **1982,** *21,* 982. (b) Burford, N.; Chivers, T.; Richardson, J. F. *Inorg. Chem.* **1983,** *22,* 1482. (c) Chivers, T.; Edwards, M.; Parvez, M. *Inorg. Chem.* **1992,** *31,* 1861.

(5) Burford, N.; Chivers, T.; Rao, M. N. S.; Richardson, J. F. *Inorg. Chem.* **1984,** *23,* 1946.

(6) Chivers, T.; Edwards, M.; Meetsma, A.; van de Grampel, J. C.; van der Lee, J. *Inorg. Chem.* **1992,** *31,* 2156.

(7) For a preliminary communication, see: Chivers, T.; Edwards, M.; Hilts, R. W.; Parvez, M.; Vollmerhaus, R. *J. Chem. Soc., Chem. Commun.* **1993,** 1483.

(8) The X-ray crystal structure of **5** is described in a preliminary communication. Chivers, T.; Edwards, M.; Hilts, R. W.; Meetsma, A.; van de Grampel, J. C. *J. Chem. Soc. Dalton Trans.* **1992,** 3053.

(9) Parshall, G. W. *Inorg. Synth.* **1970,** *12,* 27.

(10) Nagel, U. *Chem. Ber.* **1982,** *115,* 1998.

(11) Jenkins, J. M.; Verkade, J. G. *Inorg. Synth.* **1968,** *11,* 108.

0020-1669/94/1333-1440$04.50/0

$\mathrm{[SO_3CF_3]}$[12] were prepared by the literature methods. Methyllithium (1.5 M in diethyl ether), *tert*-butyllithium (1.68 M in pentane), and phenyllithium (2.0 M solution in diethyl ether/cyclohexane) were obtained from Aldrich and stored at 0 °C. Methyldiphenylphosphine was purchased from Strem Chemicals and used as received. The elemental analyses were performed by the microanalytical service within the chemistry department at The University of Calgary.

Instrumentation. Infrared spectra were recorded as Nujol mulls (KBr plates) on a Mattson 4030 FTIR spectrometer. $^{31}\mathrm{P}\ \{^1\mathrm{H}\}$ NMR spectra were recorded on a Bruker AM-400 spectrometer operating at 161.978 MHz in either THF or $\mathrm{CH_2Cl_2}$. A $\mathrm{D_2O}$ insert was used as the lock for the phosphorus spectra. Proton NMR spectra were run on either a Bruker AM-200 at 200.1 MHz or a Bruker AM-400 at 400.1 MHz, while carbon-13 NMR spectra were run on the AM-400 instrument at 100.614 MHz. For both the carbon-13 and proton-NMR spectra the solvent ($\mathrm{CDCl_3}$) deuterium resonance served as the lock. The $^{31}\mathrm{P}$ chemical shifts are reported in ppm relative to 85% $\mathrm{H_3PO_4}$; $^1\mathrm{H}$ and $^{13}\mathrm{C}$ chemical shifts are quoted relative to $\mathrm{SiMe_4}$. The $^7\mathrm{Li}\ \{^1\mathrm{H}\}$ NMR spectra were recorded on the AM-400 instrument operating at 155.508 MHz or a Varian XL-200 instrument at 77.754 MHz and the $^7\mathrm{Li}$ NMR chemical shifts are relative to 4.0 M $\mathrm{LiClO_4}$ in $\mathrm{D_2O}$. Mass spectra were recorded on a Kratos MS80 RFA instrument operated at 70 eV.

Reaction of 1,5-$\mathbf{Ph_4P_2N_4S_2}$ with Organolithium Reagents. The general procedure involved the addition of the organolithium reagent by syringe to an equimolar amount of 1,5-$\mathrm{Ph_4P_2N_4S_2}$ dissolved in THF at –78 °C. This solution was then allowed to warm to 23 °C, stirred at 23 °C for *ca.* 10 min, and then recooled to –78 °C before the addition of the electrophilic substrate. Solutions of $\mathrm{Li[Ph_4P_2N_4S_2R]}$ for variable-temperature $^7\mathrm{Li}$ and $^{31}\mathrm{P}$ NMR studies were generated in a similar manner.

Preparation of 1,5-$\mathbf{Ph_4P_2N_4S_2Me_2}$. An excess of iodomethane (0.65 mL) was added to a solution of $\mathrm{Li[Ph_4P_2N_4S_2Me]}$, generated from 1,5-$\mathrm{Ph_4P_2N_4S_2}$ (0.25 g, 0.51 mmol) and methyllithium (1.4 M in diethyl ether, 0.36 mL, 0.50 mmol), in THF (50 mL) at –78 °C. The solution was stirred for a further 1.5 h and then allowed to warm to room temperature. The solvents and excess $\mathrm{CH_3I}$ were removed under vacuum and the resulting off-white solid was washed with diethyl ether (2 × 10 mL) and dried under vacuum to give 1,5-$\mathrm{Ph_4P_2N_4S_2Me_2}$ (0.23 g, 0.44 mmol, 53%). $^{31}\mathrm{P}$ NMR (THF): 27.3(s). $^1\mathrm{H}$ NMR ($\mathrm{CDCl_3}$): 7.3–8.0 (m, $\mathrm{C_6}H_5$, 20H), 2.80 [t, $\mathrm{SC}H_3$, $^4J(\mathrm{HP})$ = 1.15 Hz, 6H], {cf. lit. 7.3–8.1 (m), 2.86 [t, $^4J(\mathrm{HP})$ = 1.4 Hz]}.[22] $^{13}\mathrm{C}$ NMR ($\mathrm{CDCl_3}$): 45.7 [t, $^3J(\mathrm{CP})$ = 21 Hz]. MS (*m/e*, %): $\mathrm{M^+}$ (520, 7), $\mathrm{M^+ - Me}$ (505, 100), $\mathrm{M^+ - 2Me}$ (490, 39). Recrystallization from $\mathrm{CH_3CN}$ gave a sample of 1,5-$\mathrm{Ph_4P_2N_4S_2Me_2}$ which contained 0.75 $\mathrm{CH_3CN}$ by integration of the $^1\mathrm{H}$ NMR resonance at 2.00 ppm. Anal. Calcd for $\mathrm{C_{26}H_{26}N_4P_2S_2{\cdot}0.75CH_3CN}$: C, 59.91; H, 5.16; N, 12.07. Found: C, 59.97; H, 5.13; N, 11.94.

Preparation of *trans*-$\mathbf{MCl(PEt_3)_2(Ph_4P_2N_4S_2R)}$. All of these complexes were prepared by using procedures similar to that described below for **4a**. The crystallizing conditions, colors and yields are summarized in this section with CHN microanalytical and $^1\mathrm{H}/^{13}\mathrm{C}$ NMR data. $^{31}\mathrm{P}$ NMR data are reported in Table 5.

Preparation of *trans*-$\mathbf{[PtCl(PEt_3)_2(\eta^1\text{-}S\text{-}Ph_4P_2N_4S_2Me)]}$, 4a. A cold solution (–78 °C) of $\mathrm{Li[Ph_4P_2N_4S_2Me]}$ in THF (20 mL), generated from 1,5-$\mathrm{Ph_4P_2N_4S_2}$ (0.100 g, 0.204 mmol) and methyllithium (1.5 M in diethyl ether, 0.14 mL, 0.210 mmol), was added by cannula to a slurry of *cis*-$\mathrm{PtCl_2(PEt_3)_2}$ (0.102 g, 0.204 mmol) in THF (20 mL) at –78 °C. The resulting yellow slurry was stirred for 30 min at –78 °C and then for 2 h at 23 °C to give a clear yellow solution. The solvents were removed under vacuum and $\mathrm{CH_2Cl_2}$ (20 mL) was added to the residue. The cloudy solution was filtered, and the clear yellow filtrate was taken to dryness under vacuum. Recrystallization of the yellow solid from hexane/THF (1:1) at 23 °C gave *trans*-$\mathrm{[PtCl(PEt_3)_2(Ph_4P_2N_4S_2Me)]}$, **4a** (0.104 g, 0.107 mmol, 52%), as pale yellow crystals. Anal. Calcd for $\mathrm{C_{37}H_{53}ClN_4P_4PtS_2}$: C, 45.70; H, 5.49; N, 5.76. Found: C, 46.12, H, 5.64; N, 5.19. $^1\mathrm{H}$ NMR ($\mathrm{CDCl_3}$, –50 °C): 7.21–7.91 (m, $\mathrm{C_6}H_5$, 20H), 2.92 [t, $\mathrm{SC}H_3$, $^4J(\mathrm{PH})$ = 1.0 Hz, 3H], 2.30 [m, $\mathrm{P(C}H_2\mathrm{CH_3)_3}$, 6H], ~1.16 [m, $\mathrm{P(C}H_2\mathrm{CH_3)_3/P(CH_2C}H_3\mathrm{)_3}$, 15H], 0.74 [dt, $\mathrm{P(CH_2C}H_3\mathrm{)_3}$, $^3J(\mathrm{PH})$ = 16 Hz, $^3J(\mathrm{HH})$ = 8 Hz, 9H]. $^{13}\mathrm{C}$ NMR ($\mathrm{CDCl_3}$, –50 °C): 127.5–136.9 (m, $C_6\mathrm{H_5}$), 44.7 [t, $\mathrm{S}C\mathrm{H_3}$, $^3J(\mathrm{PC})$ = 19 Hz], 13.2 [d, $\mathrm{P(}C\mathrm{H_2CH_3)_3}$, $^1J(\mathrm{PC})$ = 31 Hz, 11.4 [d, $\mathrm{P(}C\mathrm{H_2CH_3)_3}$, $^1J(\mathrm{PC})$ = 31 Hz], 8.3 [s, $\mathrm{P(CH_2}C\mathrm{H_3)_3}$], 7.7 [s, $\mathrm{P(CH_2}C\mathrm{H_3)_3}$]. $^{31}\mathrm{P}$ NMR data are given in Table 5.

***trans*-$\mathbf{[PtCl(PEt_3)_2(\eta^1\text{-}S\text{-}Ph_4P_2N_4S_2Bu^t)]{\cdot}CH_2Cl_2}$, 4b. 4b** was obtained as pale yellow crystals, recrystallized from $\mathrm{CH_2Cl_2}$/THF/hexane at 23 °C. Yield: 51%. Anal. Calcd for $\mathrm{C_{41}H_{61}Cl_3N_4P_4PtS_2}$: C, 44.79; H, 5.59; N, 5.10. Found: C, 45.20; H, 5.56; N, 5.22. $^1\mathrm{H}$ NMR ($\mathrm{CDCl_3}$, –35 °C): 7.25–7.89 (m, $\mathrm{C_6}H_5$, 20H), 2.42 [m, $\mathrm{P(C}H_2\mathrm{CH_3)_3}$, 6H], ~1.24 [m, $\mathrm{P(C}H_2\mathrm{CH_3)_3/P(CH_2C}H_3\mathrm{)_3}$, 15H], 1.22 [s, $\mathrm{SC(C}H_3\mathrm{)_3}$, 9H], 0.70 [dt, $\mathrm{P(CH_2C}H_3\mathrm{)_3}$, $^3J(\mathrm{PH})$ = 16 Hz, $^3J(\mathrm{HH})$ = 8 Hz, 9H]. $^{13}\mathrm{C}$ NMR ($\mathrm{CDCl_3}$, –35 °C): 127.2–138.1 (m, $C_6\mathrm{H_5}$), 55.1 [t, $\mathrm{S}C\mathrm{(CH_3)_3}$, $^3J(\mathrm{PC})$ = 15 Hz], 22.9 [s, $\mathrm{SC(}C\mathrm{H_3)_3}$], 13.2 [d, $\mathrm{P(}C\mathrm{H_2CH_3)_3}$, $^1J(\mathrm{PC})$ = 30 Hz], 11.3 [d, $\mathrm{P(}C\mathrm{H_2CH_3)_3}$, $^1J(\mathrm{PC})$ = 31 Hz], 8.2 [s, $\mathrm{P(CH_2}C\mathrm{H_3)_3}$], 7.6 [s, $\mathrm{P(CH_2}C\mathrm{H_3)_3}$].

***trans*-$\mathbf{[PtCl(PEt_3)_2(\eta^1\text{-}S\text{-}Ph_4P_2N_4S_2Ph)]}$, 4c. 4c** was obtained as pale yellow crystals, recrystallized from THF/hexane at 23 °C. Yield: 52%. Anal. Calcd for $\mathrm{C_{42}H_{55}ClN_4P_4PtS_2}$: C, 48.76; H, 5.36; N, 5.42. Found: C, 49.19; H, 5.21; N, 5.43.

***trans*-$\mathbf{[PdCl(PEt_3)_2(\eta^1\text{-}S\text{-}Ph_4P_2N_4S_2Me)]}$, 5. 5** was obtained as orange-yellow crystals, recrystallized from THF/hexane at 23 °C. Yield: 60%. Anal. Calcd for $\mathrm{C_{37}H_{53}ClN_4P_4PdS_2}$: C, 50.29; H, 6.05; N, 6.34. Found: C, 50.12; H, 5.75; N, 5.93. $^1\mathrm{H}$ NMR ($\mathrm{CDCl_3}$, –40 °C): 7.21–7.87 (m, $\mathrm{C_6}H_5$), 2.92 [t, $\mathrm{SC}H_3$, $^4J(\mathrm{PH})$ = 1.0 Hz, 3H], 2.16 [m, $\mathrm{P(C}H_2\mathrm{CH_3)_3}$, 6H], ~1.20 [m, $\mathrm{P(}C\mathrm{H_2CH_3)_3/P(CH_2C}H_3\mathrm{)_3}$, 15H], 0.77 [m, $\mathrm{P(CH_2C}H_3\mathrm{)_3}$, 9H]. $^{13}\mathrm{C}$ NMR ($\mathrm{CDCl_3}$, –35 °C): 127.4–136.2 (m, $C_6\mathrm{H_5}$), 43.2 [t, $\mathrm{S}C\mathrm{H_3}$, $^3J(\mathrm{PC})$ = 17 Hz], 13.4 [d, $\mathrm{P(}C\mathrm{H_2CH_3)}$, $^1J(\mathrm{PC})$ = 31 Hz], 12.6 [d, $\mathrm{P(}C\mathrm{H_2CH_3)_3}$, $^1J(\mathrm{PC})$ = 30 Hz], 7.9 [s, $\mathrm{P(CH_2}C\mathrm{H_3)_3}$], 7.4 [s, $\mathrm{P(CH_2}C\mathrm{H_3)_3}$].

Preparation of *trans*-$\mathbf{[PtCl(PEt_3)_2(\eta^1\text{-}S\text{-}Ph_4P_2N_4S_2CH_2PPh_2)]{\cdot}{}^1/_2CH_2Cl_2}$, 4d. *n*-Butyllithium (2.34 mL, 1.5 M solution in hexane, 3.51 mmol) was added to a stirred solution of $\mathrm{PPh_2Me}$ (0.65 mL, 3.51 mmol) and *N,N,N′,N′*-tetramethylethylenediamine (TMEDA, 0.53 mL, 3.51 mmol) in hexane (30 mL) at 23 °C. After 24 h the yellow precipitate of $\mathrm{Li(TMEDA)(CH_2PPh_2}$ was separated by decantation, washed with hexane (3 × 20 mL), and dried under vacuum for 2 h. A solution of $\mathrm{Li(TMEDA)CH_2PPh_2}$ (0.260 g, 0.807 mmol) in THF (15 mL) was added dropwise to a stirred solution of 1,5-$\mathrm{Ph_4P_2N_4S_2}$ (0.396 g, 0.807 mmol) in THF (20 mL) at –78 °C. The resulting clear yellow solution was allowed to warm up to 23 °C, stirred for 15 min, recooled to –78 °C, and then transferred via a cannula to a stirred suspension of *cis*-$\mathrm{PtCl_2(PEt_3)_2}$ (0.405 g, 0.807 mmol) in THF (20 mL) at –78 °C. The mixture was warmed to 23 °C to give a clear yellow solution after 2 h. The solvent was removed under vacuum, the residue was extracted with benzene (20 mL), and the precipitate of LiCl was removed by filtration. Removal of benzene from the filtrate under vacuum gave a yellow residue, which was recrystallized from $\mathrm{CH_2Cl_2}$/hexane at 23 °C to give yellow microcrystals of *trans*-$\mathrm{[PtCl(PEt_3)_2(\eta^1\text{-}S\text{-}Ph_4P_2N_4S_2CH_2PPh_2)]{\cdot}{}^1/_2CH_2Cl_2}$ (0.288 g, 0.240 mmol, 30%). Anal. Calcd for $\mathrm{C_{49.5}H_{63}Cl_2N_4P_5PtS_2}$: C, 49.58; H, 5.30; N, 4.67. Found: C, 49.82; H, 4.57; N, 4.08.

Reaction of $\mathbf{Li[Ph_4P_2N_4S_2Me]}$ with *cis*-$\mathbf{PtCl_2(PPh_3)_2}$. A pale yellow solution of $\mathrm{Li[Ph_4P_2N_4S_2Me]}$ (0.249 mmol) in THF (20 mL) at –78 °C was added by cannula to a slurry of *cis*-$\mathrm{PtCl_2(PPh_3)_2}$ (0.197 g, 0.249 mmol) in THF at –78 °C. The resulting yellow slurry was gradually warmed to 65 °C to give a golden yellow solution. After 1 h at 65 °C, the solvent was removed under vacuum to give a deep yellow solid. The $^{31}\mathrm{P}\ \{^1\mathrm{H}\}$ NMR spectrum of this solid in $\mathrm{CH_2Cl_2}$ revealed the presence of two compounds, $\mathrm{[Pt(PPh_3)_2(\eta^2\text{-}S,S'\text{-}Ph_4P_2N_4S_2)]}$[6] [$\delta(^{31}\mathrm{P})$ ($\mathrm{CH_2Cl_2}$): 17.8 [t, $P\mathrm{Ph_3}$, $^4\mathrm{J(PP)}$ = 5 Hz, $^1\mathrm{J(PtP)}$ = 2861 Hz], 37.7 [t, $P_2\mathrm{N_4S_2}$, $^4\mathrm{J(PP)}$ = 5 Hz, $^3\mathrm{J(PtP)}$ = 580 Hz]] and $\mathrm{[Pt(\eta^1\text{-}THF\text{-}}O\mathrm{)(PPh_3)(\eta^2\text{-}Ph_4P_2N_4S_2\text{-}}S,S'\mathrm{)]}$, 7 [$\delta(^{31}\mathrm{P})$ ($\mathrm{CH_2Cl_2}$): 31.4 [d, $P_2\mathrm{N_4S_2}$, $^4J(\mathrm{PP})$ = 5 Hz, $^3J(\mathrm{PtP})$ = 425 Hz], 18.8 [t, $P\mathrm{Ph_3}$, $^4J(\mathrm{PP})$ = 5 Hz, $^1\mathrm{J(PtP)}$ = 3228 Hz]] in *ca.* a 2:3 ratio.

X-ray Structural Analysis. Crystals of $\mathrm{[Li(Ph_4P_2N_4S_2Ph){\cdot}THF]_2}$ were obtained as colorless blocks from a THF–diethyl ether solution. All measurements were made on a Rigaku AFC6S diffractometer with graphite-monochromated Mo Kα radiation on a crystal with approximate dimensions 0.70 × 0.35 × 0.20 mm. Accurate cell constants and an orientation matrix were obtained from a least-squares refinement of the setting angles of 25 reflections in the range $22.97 < 2\theta < 36.37°$. Intensity data were collected by the $\omega/2\theta$ scan method. Scans of $(1.47 + 0.34 \tan\theta)°$ were made at a speed of 8.0° $\mathrm{min^{-1}}$. Of the 6232 reflections collected, 5950 were unique (R_int = 0.060). The intensities of three representative reflections were measured after every 200 reflections. Over the course of data collection, the standards decreased by 0.8%. A linear correction factor was applied to the data to account for this decay. An empirical absorption correction using the program DIFABS[13] was applied which resulted in transmission factors ranging from 0.77 to 1.14. The data

---

(12) Chivers, T., Dénès, G. Y.; Liblong, S. W.; Richardson, J. F. *Inorg. Chem.* **1989**, *28*, 3683.

(13) Walker, N.; Stuart, D. *Acta Crystallogr.* **1983**, *A39*, 158.

Table 1. Crystallographic Data for $[Li(Ph_4P_2N_4S_2Ph)\cdot THF]_2$

formula	$C_{34}H_{33}P_2N_4S_2LiO$	V, Å^3	1683(2)
fw	646.67	Z	2
space group	$P\bar{1}$ (No. 2)	T, K	296
a, Å	13.189(10)	λ, Å	0.710 69
b, Å	13.335(8)	ρ_{calcd}, g cm^{-3}	1.276
c, Å	11.760(5)	μ, mm^{-1}	0.286
α, deg	90.67(4)	R^a	0.072
β, deg	114.15(4)	$R_w{}^b$	0.060
γ, deg	114.05(5)		

[a] $R = \sum||F_o| - |F_c||/\sum|F_o|$. [b] $R_w = [\sum w\delta^2/\sum wF_o{}^2]^{1/2}$.

Table 2. Atomic Coordinates for $[Li(Ph_4P_2N_4S_2Ph)\cdot THF]_2$ with Esd's in Parentheses

atom	x	y	z	B_{eq},[a] Å^2
S(1)	−0.0092(3)	0.1680(3)	−0.0155(3)	3.21(9)
S(2)	−0.1285(3)	0.2195(3)	−0.3025(3)	3.06(8)
P(1)	0.1212(3)	0.2921(3)	−0.1375(3)	3.04(9)
P(2)	−0.2233(3)	0.0216(3)	−0.2239(3)	2.74(9)
O(1)	0.0766(10)	−0.0358(9)	−0.2175(9)	5.9(3)
N(1)	0.1147(9)	0.2003(8)	−0.0485(9)	3.5(3)
N(2)	−0.1048(8)	0.0265(7)	−0.0951(9)	2.7(3)
N(3)	−0.2022(9)	0.0846(7)	−0.3339(8)	3.1(3)
N(4)	0.0116(9)	0.2621(8)	−0.2813(9)	3.3(3)
C(1)	0.2547(12)	0.3263(10)	−0.1597(13)	3.3(4)
C(2)	0.3651(13)	0.3367(11)	−0.0588(13)	4.5(4)
C(3)	0.4721(15)	0.3646(13)	−0.0698(17)	6.1(5)
C(4)	0.4776(17)	0.3828(14)	−0.1795(22)	7.3(7)
C(5)	0.3695(18)	0.3708(15)	−0.2797(18)	7.3(6)
C(6)	0.2604(14)	0.3429(12)	−0.2696(15)	5.7(5)
C(7)	0.1477(12)	0.4233(10)	−0.0530(13)	3.7(4)
C(8)	0.1419(15)	0.5103(12)	−0.1146(14)	5.7(5)
C(9)	0.1560(18)	0.6053(13)	−0.0568(19)	8.0(6)
C(10)	0.1738(16)	0.6176(14)	0.0665(20)	7.1(6)
C(11)	0.1823(17)	0.5345(14)	0.1331(16)	6.7(6)
C(12)	0.1695(13)	0.4414(11)	0.0758(14)	4.7(4)
C(13)	−0.3176(11)	−0.1255(10)	−0.3054(12)	3.2(3)
C(14)	−0.3189(14)	−0.2103(12)	−0.2437(13)	6.1(4)
C(15)	−0.4017(16)	−0.3221(11)	−0.3048(15)	6.8(5)
C(16)	−0.4813(16)	−0.3460(12)	−0.4296(15)	6.8(5)
C(17)	−0.4818(16)	−0.2632(12)	−0.4941(13)	6.7(5)
C(18)	−0.4003(15)	−0.1516(11)	−0.4317(13)	5.9(4)
C(19)	−0.3173(11)	0.0635(9)	−0.1756(12)	2.8(3)
C(20)	−0.4024(13)	0.0923(11)	−0.2599(13)	4.1(4)
C(21)	−0.4756(13)	0.1207(12)	−0.2266(14)	5.0(5)
C(22)	−0.4648(14)	0.1241(12)	−0.1038(16)	5.2(5)
C(23)	−0.3753(13)	0.0956(13)	−0.0165(14)	4.8(4)
C(24)	−0.3068(12)	0.0648(11)	−0.0540(13)	4.1(4)
C(25)	−0.1943(12)	0.2497(10)	−0.4587(12)	3.6(3)
C(26)	−0.3030(12)	0.1725(11)	−0.5565(13)	4.2(4)
C(27)	−0.3567(13)	0.2011(14)	−0.6729(13)	6.1(5)
C(28)	−0.3009(15)	0.3092(14)	−0.6835(15)	7.3(5)
C(29)	−0.1936(18)	0.3878(15)	−0.5859(17)	11.4(6)
C(30)	−0.1401(16)	0.3599(13)	−0.4737(16)	8.3(6)
C(31)	0.146(2)	0.026(2)	−0.277(2)	11.3(8)
C(32)	0.142(3)	−0.045(2)	−0.366(2)	15(1)
C(33)	0.033(3)	−0.156(2)	−0.389(3)	19(1)
C(34)	−0.012(3)	−0.140(2)	−0.304(2)	16.8(10)
Li(1)	0.056(2)	0.028(2)	−0.078(2)	3.5(6)

[a] $B_{eq} = {}^8/_3\pi^2(U_{11}(aa^*)^2 + U_{22}(bb^*)^2 + U_{33}(cc^*)^2 + 2U_{12}aa^*bb^* \cos\gamma + 2U_{13}aa^*cc^* \cos\beta + 2U_{23}bb^*cc^* \cos\alpha)$.

were corrected for Lorentz and polarization effects. Crystal data are given in Table 1.

The structure was solved and expanded by using Fourier techniques.[14] The non-hydrogen atoms were refined anisotropically. Hydrogen atoms were included but not refined. The refinement converged with $R = 0.072$ and $R_w = 0.060$. The final values of the refined positional parameters are given in Table 2. The weighting scheme was based on counting statistics and including a factor ($p = 0.002$) to downweight the intense reflections. Neutral atom scattering factors were taken from Cromer and Waber.[15] Anomalous dispersion effects were included in F_{calc};[16] the values of $\Delta f'$ and $\Delta f''$ were those of Creagh and McAuley.[17] The values for the mass attenuation coefficients were those of Creagh and Hubbell.[18] All calculations were performed using teXsan.[19]

Results and Discussion

Reaction of 1,5-$Ph_4P_2N_4S_2$ with Organolithium Reagents. The addition of methyllithium to a solution of 1,5-$Ph_4P_2N_4S_2$, **1a**, in THF at −78 °C, followed by warming to room temperature, produces a soluble species which, on the basis of its derivative chemistry, is identified as the lithium complex of the methylated anion $Ph_4P_2N_4S_2Me^-$. For example, the treatment of this anion with an excess of iodomethane produces the *S,S'*-dimethyl derivative 1,5-$Ph_4P_2N_4S_2Me_2$, **2**, in 53% yield (Scheme 1). The structures of the related compounds 1,5-$Ph_4P_2N_4Se_2Me_2$[20] and 1,5-$Ph_4P_2N_4S_2Ph_2$[21] have been shown by X-ray crystallography to involve an eight-membered chair with the two chalcogen atoms displaced on opposite sides of the P_2N_4 plane. The heterocycle **2** has previously been prepared from $(Ph_2PN)_2SMe_2$ and the explosive reagent $Me_2S(NBr)_2$[22] and by the reaction of $Li_2[Ph_4P_2N_4S_2]$ with 2 molar equiv of iodomethane.[23] In this work it was shown by ^{31}P NMR spectroscopy that **2** can also be generated readily by treatment of the N-methylated cationic derivative of **1a**, $[Ph_4P_2N_4S_2Me][CF_3SO_3]$,[12] with methyllithium (Scheme 1). Thus the reaction with methyl-lithium induces a [1,2] (N → S) methyl shift.

The substituents on phosphorus have a marked effect on the susceptibility of the $P_2N_4S_2$ ring in **1** to nucleophilic attack. Although **1a** reacts readily with a variety of organolithium reagents at 25 °C in THF, the corresponding tetraalkyl derivatives **1b** and **1c** are unaffected. A similar disparity was found for the reactions of **1a–c** with $Li[BEt_3H]$ in THF.[23] Whereas **1a** reacts to form $Li_2[Ph_4P_2N_4S_2]$, **1b** and **1c** undergo no reaction with Super-hydride (Aldrich).[24] Furthermore, there are limitations on the type of organolithium reagent that reacts with **1a**. While MeLi, Bu^tLi, PhLi and Ph_2PCH_2Li all react readily with **1a** (eq 1), the reagents $LiNPr_2{}^i$ and $LiC{\equiv}CR$ (R = H, $SiMe_3$) do not react.

$$1,5\text{-}Ph_4P_2N_4S_2 + LiR \xrightarrow[-78\ ^\circ C]{THF} \underset{3}{Li[Ph_4P_2N_4S_2R]} \qquad (1)$$

3a, R = Me; **3c**, R = Ph; **3b**, R = ^tBu; **3d**, R = CH_2PPh_2

The reactions of **1a–c** with electrophiles invariably produce N-bonded adducts.[12,24] By contrast, nucleophilic attack is expected to occur at sulfur via the antibonding σ*(S–S) orbital of **1**.[25] This expectation was confirmed by the X-ray structure of (**3c**·THF)$_2$.

---

(14) Beurskens, P. T.; Admiraal, G.; Beurskens, G.; Bosman, W. P.; Garcia-Garcia, S.; Gould, R. O.; Smits, J. M. M.; Smykalla, C. The DIRDIF program system. Technical Report of the Crystallography Laboratory, University of Nijmegen, The Netherlands, 1992.

(15) Cromer, T.; Waber, J. T. *International Tables for Crystallography*; The Kynoch Press, Birmingham, England, 1974; Vol. IV, Table 2.2A.

(16) Ibers, J. A.; Hamilton, W. C. *Acta Crystallogr.* **1964**, *17*, 781.

(17) Creagh, D. C.; McAuley, W. J. In *International Tables for Crystallography*; Wilson, A. J. C., Ed.; Kluwer Academic Publishers: Boston, MA, 1992; Vol. C, Table 4.2.6.8.

(18) Creagh, D. C.; Hubbell, J. H. In *International Tables for Crystallography*; Wilson, A. J. C., Ed.; Kluwer Academic Publishers: Boston, MA, 1992; Vol. C, Table 4.2.4.3.

(19) teXsan: Crystal Structure Analysis Package. Molecular Structure Corp., 1985 and 1992.

(20) Chivers, T.; Doxsee, D. D.; Fait, J. F. *J. Chem. Soc., Chem. Commun.* **1989**, 1703.

(21) Chivers, T.; Kumaravel, S. S.; Meetsma, A.; van de Grampel, J. C.; van der Lee, A. *Inorg. Chem.* **1990**, *29*, 4591.

(22) Appel, R.; Eichenhofer, K. W. *Chem. Ber.* **1971**, *104*, 3859.

(23) Chivers, T.; Cowie, M.; Edwards, M.; Hilts, R. W. *Inorg. Chem.* **1992**, *31*, 3349.

(24) The substituents on phosphorus have also obeen shown to influence the Lewis basicity of the $P_2N_4S_2$ ring. The tetraalkyl derivatives, **1b** and **1c**, form stronger N-bonded complexes with platinum(II) than **1a**. Chivers, T.; Hilts, R. W. *Inorg. Chem.* **1992**, *31*, 5272.

(25) Jacobson, H.; Ziegler, T.; Chivers, T.; Vollmerhaus, R. *Can. J. Chem.*, in press.

Scheme 1. Preparation of 1,5-$Ph_4P_2N_4S_2Me_2$, **2**: (i) MeLi, (ii) $MeSO_3CF_3$, (iii) MeI

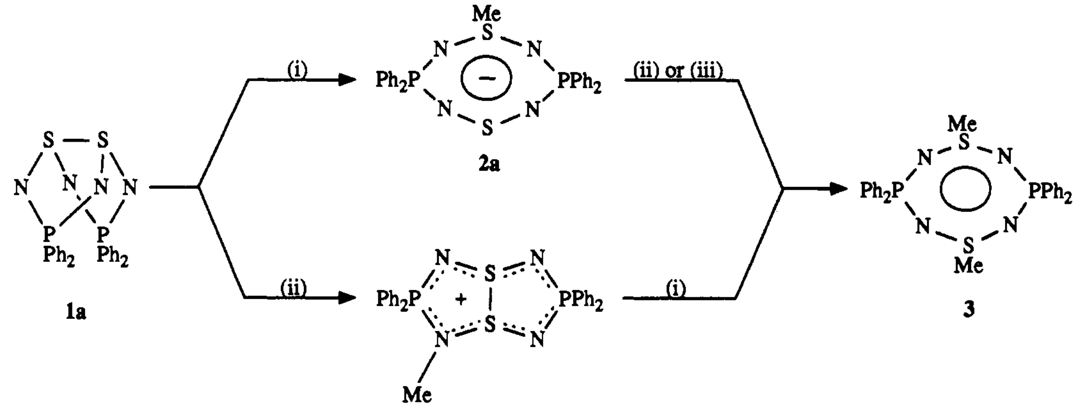

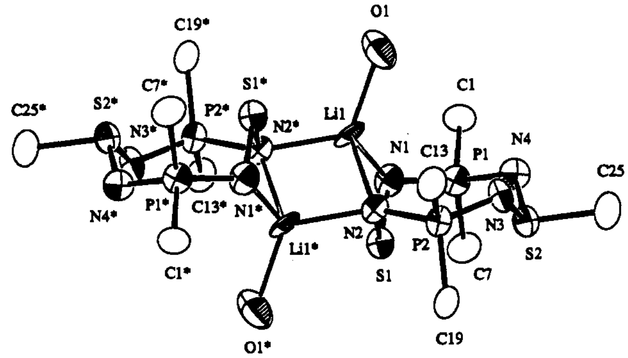

Figure 1. ORTEP drawing (50% probability ellipsoids) for [Li-($Ph_4P_2N_4S_2Ph$)·THF]$_2$, (**3c**·THF)$_2$.

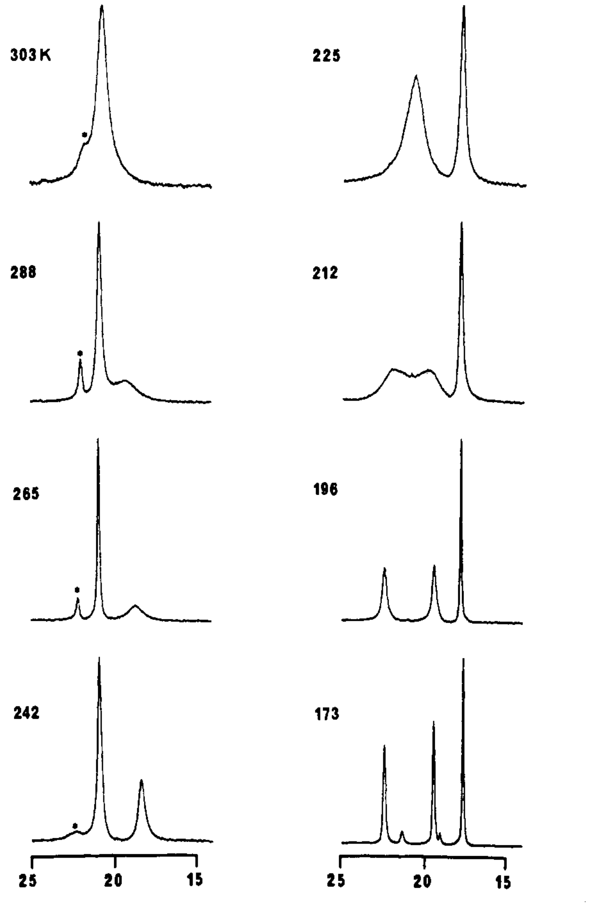

Figure 2. ^{31}P NMR spectra of an equimolar mixture of 1,5-$Ph_4P_2N_4S_2$, **1a**, and methyllithium in THF at various temperatures. The species responsible for the signal designated with an asterisk (*) has not been identified.

X-ray Structure of [Li($Ph_4P_2N_4S_2Ph$)·THF]$_2$. The molecular geometry and atomic numbering scheme for (**3c**·THF)$_2$ are depicted in Figure 1. The attachment of the phenyl group to sulfur results in the loss of the transannular S--S interaction [*d*(S–S) = 3.31(1) Å] and causes the $P_2N_4S_2$ ring to adopt a boat conformation (*cf.* the chair conformation for the *S,S'*-diphenyl derivative 1,5-$Ph_4P_2N_4S_2Ph_2$).[21] The molecule is a centrosymmetric dimer with a ladder structure similar to that established for certain organolithium derivatives of $Me_3SiNSNSiMe_3$.[26,27] However, in contrast to the structure of [$(Me_3SiN)_2S$(Ph)-Li·THF]$_2$, in which the lithium atoms are bonded *asymmetrically* to NSN units,[27] each lithium atom in (**3c**·THF)$_2$ is attached almost symmetrically to two vicinal nitrogen atoms of one $P_2N_4S_2$ ring [*d*(Li–N) = 2.03(2) and 2.08(2) Å] and forms a bridge to one nitrogen atom of the other $P_2N_4S_2$ ring [*d*(Li–N) = 2.10(2) Å]. A single THF molecule completes the coordination sphere of each lithium atom. Coordination to lithium has a pronounced effect on the S–N bond lengths in **1a** which increase from 1.62 Å[4b] to 1.72(1) and 1.755(9) Å in (**3c**·THF)$_2$ suggesting that organolithium reagents might be used to promote ring opening of **1a**. For comparison, we note that the reaction of S_4N_4 with *n*-butyllithium results in a ring contraction to give $S_3N_3^-$.[3]

As a result of the different coordination modes of the nitrogen atoms N(1) and N(2) in (**3c**·THF)$_2$, the phosphorus atoms of each $P_2N_4S_2$ ring are inequivalent. Consequently, ^{31}P NMR spectroscopy should provide an informative probe of the solution structure of (**3c**·THF)$_2$ and related derivatives. The results of such NMR investigations are described below.

Solution Structures and Fluxional Behavior of [Li($Ph_4P_2N_4S_2R$)]$_2$. The ^{31}P NMR spectra of a solution of [Li($Ph_4P_2N_4S_2Me$)]$_2$ (**3a**)$_2$ in THF at various temperatures are illustrated in Figure 2. The ^{31}P NMR spectrum consists of a broad singlet at room temperature, indicating that a fluxional process is occurring. Surprisingly, when the solution is cooled to 173 K *three* distinct resonances are observed: two singlets of equal intensity at 22.5 and 19.5 ppm, and a third singlet at 17.8 ppm. When the temperature of the solution is raised gradually to 242 K, the two signals at high frequency broaden simultaneously and eventually collapse to give one averaged resonance at 20.5 ppm. The same pattern of behavior is observed for THF solutions of (**3b**)$_2$, (**3c**)$_2$ and (**3d**)$_2$ in this temperature range (see Table 3). These observations are consistent with the presence of a dimer, with a structure similar to that of (**3c**·THF)$_2$, which undergoes a rapid fluxional process above *ca.* 240 K. Coalescence for the two-site exchange for the unsymmetrical dimers (**3a**–**d**·THF)$_2$ occurs in the temperature range 210–220 K with activation

---

(26) Pauer, F.; Stalke, D. *J. Organomet. Chem.* **1991**, *418*, 127.
(27) Edelmann, F. T.; Knösel, F.; Pauer, F.; Stalke, D.; Bauer, W. *J. Organomet. Chem.* **1992**, *438*, 1.

Table 3. $^{31}P\{^1H\}$ NMR Parameters for $[Li(Ph_4P_2N_4S_2R)]_2$ (R = Me, Bu^t, Ph, CH_2PPh_2)[a,b]

	$\delta(P_A)$[c]	$\delta(P_B)$[c]	$\delta(P_A/P_B)$[d]	*T*[e]	E_A[f]	$\delta(P_C)$[g]
(**3a**)$_2$	22.5	19.5	20.5	213 ± 2	32.6 ± 1	17.8
(**3b**)$_2$	21.9	20.3	21.1	210 ± 2	33.9 ± 1	17.7
(**3c**)$_2$	24.5	21.6	23.1	220 ± 2	35.5 ± 1	19.5
(**3d**)$_2$	23.3	21.0	22.4	*ca.* 215	h	18.9

[a] Chemical shifts are quoted in ppm relative to 85% H_3PO_4. [b] Spectra were recorded in THF-d_8 or THF with acetone-d_6 external lock and chemical shifts were determined at *ca.* 173 K. [c] P_A and P_B represent the inequivalent phosphorus atoms of the unsymmetrical dimers. The assignments are arbitrary. [d] Chemical shift of the coalesced resonances P_A and P_B. [e] Coalescence temperature in K. [f] Activation energy in kJ mol^{-1}.[28] [g] P_C represents the phosphorus atoms of the symmetrical dimer. [h] Not determined.

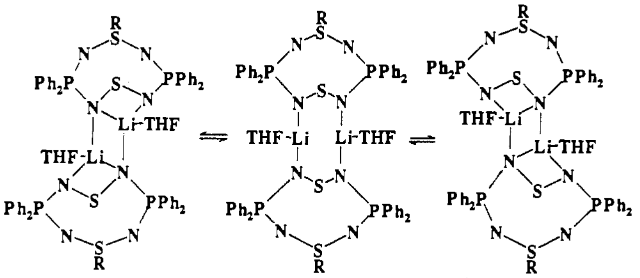

Figure 3. Proposed two-site exchange process for $[Li(Ph_4P_2N_4S_2R)]_2$ in THF (R = Me, Bu^t, Ph, CH_2PPh_2).

energies of 32.6–35.5 ± 1 kJ mol^{-1} (see Table 3).[28] This two-site exchange process could occur via a symmetrical eight-membered $Li_2N_4S_2$ ring (see Figure 3) of the type that has been established in the solid state for $[(Me_3SiNS(Bu^t)NBu^t)Li]_2$.[26] In this process, the lithium atoms rock back and forth between $P_2N_4S_2$ rings. We note that the corresponding cation $Ph_4P_2N_4S_2Me^+$ is static on the NMR time scale at room temperature, as indicated by the observation of two resonances in the ^{31}P NMR spectrum.[12] However, the folded ring structure of **1a** is retained in the methylated cation (see Scheme 1).

The third resonance, which is observed as a singlet ($\delta(^{31}P)$ = 18–20 ppm) at 173 K in the ^{31}P NMR spectra of (**3a–d**)$_2$ in THF, is attributed to a species with equivalent phosphorus atoms (P_C in Table 3). Significantly, the ^{31}P NMR spectrum of (**3d**)$_2$ in THF at 173 K exhibits only two resonances, at -30.2 and -30.6 ppm, for the exocyclic CH_2PPh_2 group. Integration of this ^{31}P NMR spectrum reveals that the area of the resonance at -30.2 ppm is equal to the combined area of the two signals at 21.0 and 23.3 ppm assigned to (**3d**·THF)$_2$, and the area of the resonance at -30.6 ppm is approximately half that of the singlet at 18.9 ppm attributed to the symmetrical species. These observations are consistent with the contention that only two species are present in solution. Furthermore, the ^7Li NMR spectra of solutions of (**3a–c**)$_2$ in THF at 200 K exhibit only two resonances (see Table 4) indicating the presence of two species (the lithium sites in the dimer (**3c**·THF)$_2$ are equivalent).

What is the nature of the symmetrical species? The changes that occur in the ^{31}P and ^7Li NMR spectra as a function of concentration are informative. The intensity of the ^{31}P NMR resonances of the unsymmetrical dimers (**3a-c**·THF)$_2$ decreases relative to that of the resonance at 18–20 ppm with dilution of the THF solution, and at ca. 13 mM only the latter resonance is observed at 185 K. This suggests that the symmetrical species is either a monomer or a more highly solvated dimer with equivalent phosphorus atoms. Consistently, the relative intensity of the ^7Li NMR resonances at low field decreases with dilution, and at 13 mM this resonance is no longer observed. Thus this resonance is attributed to the unsymmetrical dimers (**3a–c**·THF)$_2$. We note, however, that the resonance for the symmetrical species collapses in both the ^{31}P (see Figure 2) and ^7Li NMR spectra (see Figure 4) when the temperature is raised from *ca.* 230 to 330 K. This is incompatible with a monomeric structure, since dissociation to a monomer should be favoured by an increase in temperature. We propose, therefore, that this species is a dimer involving an eight-membered $Li_2N_4S_2$ ring (see middle structure of Figure 3), but with each lithium atom coordinated to two THF molecules i.e. $[Li(Ph_4P_2N_4S_2R)(THF)_2]_2$. The increase in the relative intensities of the ^7Li and ^{31}P NMR resonances of this species upon dilution is consistent with this suggestion while the disappearance of these resonances with an increased in temperature (for a given concentration) is ascribed to the dissociation of one THF molecule (per lithium atom) to give the unsymmetrical dimers (**3a–c**·THF)$_2$. Variation in the degree of solvation of dimeric structures is a well-established feature of the solution structures of organonitrogen–lithium compounds.[29,30]

Table 4. ^7Li $\{^1H\}$ NMR Parameters for $[Li(Ph_4P_2N_4S_2R)]_2$ in THF[a,b]

	$\delta(^7Li)$	*T*, K
(**3a**)$_2$	0.56(s), 1.03(s)	200
	1.01(s)	300
(**3b**)$_2$	0.02(s), 0.78(s)	200
	0.41(s)	300
(**3c**)$_2$	0.35(s), 0.98(s)	200
	0.47(s)	300

[a] Chemical shifts are quoted in ppm relative to 4.0 M $LiClO_4$ in D_2O. [b] Spectra were recorded in THF, with toluene-d_8 insert. The high-field signal is assigned to $[Li(Ph_4P_2N_4S_2R)(THF)_2]_2$, and the low-field signal is ascribed to $[Li(Ph_4P_2N_4S_2R)(THF)]_2$.

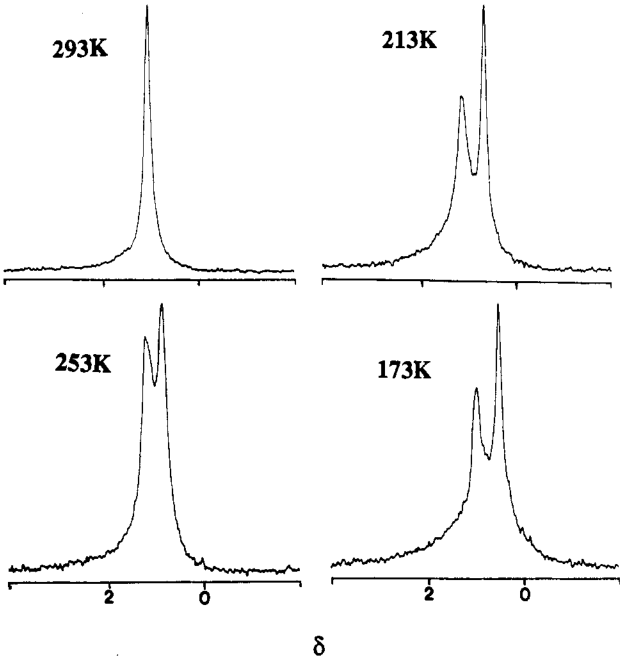

Figure 4. ^7Li NMR spectra of a 58 mM solution of $[Li(Ph_4P_2N_4S_2Me)THF]_2$ in THF at various temperatures.

Support for this interpretation of the species present in THF solution is provided by the variable-temperature ^7Li and ^{31}P NMR spectra of (**3c**·THF)$_2$ in toluene. The ^{31}P NMR spectrum of (**3c**·THF)$_2$ in toluene at 200 K exhibits only two resonances at 21.8 and 22.2 ppm. As the temperature of this solution is increased, these resonances broaden and collapse at *ca.* 235 K to yield a single, relatively narrow resonance with a chemical shift of 21.7 ppm at 300 K. The ^7Li NMR spectrum of (**3c**·THF)$_2$

---

(28) Sandström, J. *Dynamic NMR Spectroscopy*; Academic Press: New York, 1982.

(29) Gregory, K.; Schleyer, P. von R.; Snaith, R. *Adv. Inorg. Chem.* **1991**, *37*, 47.

(30) Jackman, L. M.; Scarmoutzos, L. M. *J. Am. Chem. Soc.* **1987**, *109*, 5348.

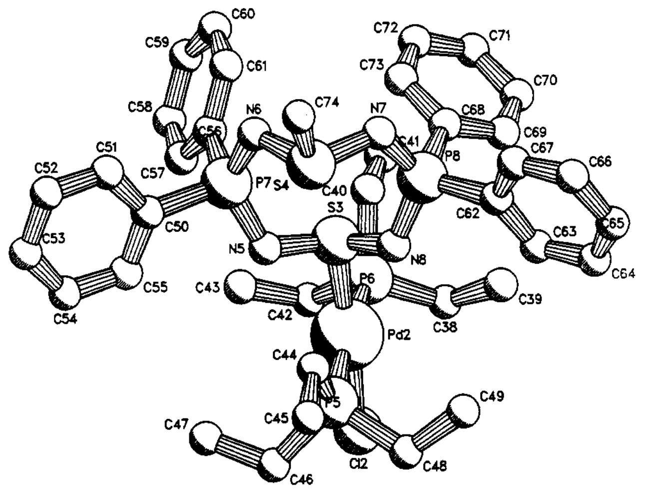

Figure 5. PLUTO drawing of the structure of **5** (M = Pd).

in toluene at 200 K shows only a single resonance at 0.85 ppm, which undergoes a temperature-dependent shift to 1.1 ppm upon raising the temperature to 300 K. These observations indicate that, in the absence of an excess of THF, a single, monosolvated species ($\mathbf{3c}\cdot$THF)$_2$, unsymmetrical with respect to phosphorus atoms but symmetrical with respect to lithium atoms, is present in solution.

Preparation and Structure of *trans*-MCl(PEt$_3$)$_2$(η^1-S-Ph$_4$P$_2$N$_4$S$_2$R). The neutral 1,5-diphosphadithiatetrazocines **1a–c** exhibit a versatile coordination chemistry involving sulfur and/or nitrogen ligation to metals.[31] It was of interest, therefore, to investigate the coordination behavior of the anionic ligands $Ph_4P_2N_4S_2R^-$. To date, the following bonding modes have been established for the $P_2N_4S_2$ ring: η^1-N,[24] η^2-S,S',[6] μ,η^2(N,S):η^1(S'),[6] and μ,η^3(N,N',S):η^1(S').[32] The reactions of the lithium derivatives of the anions $Ph_4P_2N_4S_2R^-$ with *cis*- or *trans*-PtCl$_2$(PEt$_3$)$_2$ and *trans*-PdCl$_2$(PEt$_3$)$_2$ proceed rapidly above 0 °C in THF to give good yields of **4a–d** and **5** as air-stable yellow or orange solids (eq 2). The fact that the *trans*-complexes are obtained from either *cis*- or *trans*-PtCl$_2$(PEt$_3$)$_2$ indicates a thermodynamic preference for this geometry.

$$\mathrm{Li[Ph_4P_2N_4S_2R]} + cis\text{- or } trans\text{-}\mathrm{MCl_2(PEt_3)_2} \rightarrow trans\text{-}\mathrm{MCl(PEt_3)_2(Ph_4P_2N_4S_2R)} \quad (2)$$

4a–d, 5

R = Me, Bu^t, Ph, CH$_2$PPh$_2$; M = Pt, Pd

4a, R = Me, M = Pt; **4b**, R = Bu^t, M = Pt; **4c**, R = Ph, M = Pt; **4d**, R = CH$_2$PPh$_2$, M = Pt; **5**, R = Me, M = Pd

The structure of the palladium derivative **5** was determined by X-ray crystallography. Details have been given in the preliminary communication of this work[8] and will not be repeated here. A PLUTO drawing of the structure is illustrated in Figure 5 to accompany the discussion of stereochemical nonrigidity. One of the sulfur atoms of the $P_2N_4S_2$ ring in **5** is attached to a methyl group while the other is bonded to an approximately square planar palladium atom. The $P_2N_4S_2$ ring tends toward a chair conformation. The PEt$_3$ ligands are *trans* to each other and the square plane of coordination about palladium bisects the $P_2N_4S_2$ ring (through the S–S vector). In this orientation the Ph$_2$P groups of the heterocyclic ring are equivalent, but the PEt$_3$ ligands are inequivalent.

Table 5. ^{31}P {^{1}H} NMR Parameters for MCl(PEt$_3$)$_2$(Ph$_4$P$_2$N$_4$S$_2$R)[a,b]

	4a	**4b**	**4c**	**4d**	**5**
$\delta(P_A)^c$	21.4	20.2	21.8	19.4	20.1
$\delta(P_B)^c$	15.5	14.2	15.5	13.8	16.8
$\delta(P_C)^d$	27.1	27.0	29.0	24.5	24.8
$^2J(P_AP_B)^c$	388	389	388	383	388
$^4J(P_CP_A)^d$	~0	~0	3	~0	17.5
$^4J(P_CP_B)^d$	~0	~0	~2	~0	11
$^1J(PtP_A)$	2963	2969	2920	2924	
$^1J(PtP_B)$	2676	2683	2679	2677	
$^3J(PtP_C)$	464	456	472	484	
$\delta(CH_2PPh_2)$				−30.7(s)	

[a] Chemical shifts are quoted in ppm relative to 85% H$_3$PO$_4$; coupling constants are reported in Hz. [b] Spectra were recorded at *ca.* 223 K in toluene-d_8 for **4a–c** and **5** and in CH$_2$Cl$_2$ with external D$_2$O lock for **4d**. [c] P$_A$ and P$_B$ represent the phosphorus atoms of inequivalent PEt$_3$ ligands, i.e. P(5) and P(6) in Figure 5. The assignments of P$_A$ and P$_B$ are arbitrary. The resonances for P$_A$ and P$_B$ appear as an AB quartet at 223 K. [d] P$_C$ represents the phosphorus atoms of equivalent PPh$_2$ groups, i.e. P(7) and P(8) in Figure 5. The resonance for P$_C$ in **5** is an overlapping doublet of doublets due to coupling to both P$_A$ and P$_B$; these couplings are not resolved in the signal for P$_C$ in **4a**, **4b**, and **4d** which is a singlet for all three derivatives.

Low-Temperature ^{31}P NMR Spectra of *trans*-MCl(PEt$_3$)$_2$(η^1-S-Ph$_4$P$_2$N$_4$S$_2$R), 4a–d and 5. The ^{31}P NMR spectrum of **5** at *ca.* 223 K (Table 5) is consistent with the structure depicted in Figure 5. The resonances for the inequivalent PEt$_3$ ligands appear as an AB quartet, with fine structure, having chemical shifts of 16.8 and 20.1 ppm and a mutual coupling of 388 Hz, typical for *trans* PEt$_3$ groups attached to Pd.[33] The equivalent PPh$_2$ groups give rise to a singlet at 24.8 ppm, and they are involved in three-bond couplings of 17.5 and 11 Hz to the inequivalent PEt$_3$ ligands. The ^{31}P NMR spectra of the platinum complexes **4a–d** display features very similar to that of **5** with additional information provided from Pt–P coupling constants. Thus the inequivalent PEt$_3$ ligands exhibit an AB quartet with chemical shifts of 19–22 and 14–16 ppm, respectively. The corresponding ^1J(PtP) values are in the ranges 2675–2685 and 2920–2970 Hz, respectively, typical for trialkylphosphine ligands *trans* to each other in a platinum(II) complex.[33] The resonances for the equivalent PPh$_2$ groups of **4a–d** occur at 24–29 ppm and exhibit a three-bond coupling to ^{195}Pt of 455–485 Hz. These coupling constants are comparable to the value of 585 Hz observed for ^3J(PPt) in Pt(PPh$_3$)$_2$(η^2-Ph$_4$P$_2$N$_4$S$_2$-*S,S'*).[6] The four-bond P–P couplings between the heterocyclic phosphorus atoms and the phosphorus atoms of the PEt$_3$ ligands are not observed for the Pt complexes. On the basis of these ^{31}P NMR data we conclude that the static structures of the platinum complexes **4a–d** are similar to that of the palladium complex, **5**.

Stereochemical Nonrigidity of 4a–c and 5. When the temperature of solutions of **4a–c** or **5** is raised from 223 to 303 K, the AB quartet for the inequivalant PEt$_3$ ligands collapses and then appears as a singlet (with ^{195}Pt satellites for **4a–c**) while the resonance for the equivalent PPh$_2$ groups remains essentially unaffected. This behavior is illustrated by a representative example, **5**, in Figure 6. These changes are reversible upon recooling the solutions to 223 K. In all cases the single resonance for the two PEt$_3$ ligands at the fast exchange limit is located at the mean of the chemical shifts for these two groups at 223 K, and the ^1J(PtP) coupling constant at the fast exchange limit for **4a–c** is the average of those observed at 223 K. Furthermore, the one-bond Pt–P coupling is maintained throughout the temperature range, indicating that the stereochemical nonrigidity of these complexes involves an intramolecular two-site exchange. There are two possible explanations of this behavior. The first involves a simple rotation of the $P_2N_4S_2$ ligand about the metal–

---

(31) Chivers, T.; Hilts, R. W. *Coord. Chem. Rev.*, in press.

(32) Chivers, T.; Hilts, R. W. Parvez, M.; Hofmann, K.; Ristic-Petrovic, D.; *J. Organomet. Chem.*, submitted for publication.

(33) See, for example: Berry, D. E.; Browning, J.; Dixon, K. R.; Hilts, R. W. *Can. J. Chem.* **1988**, *66*, 1272.

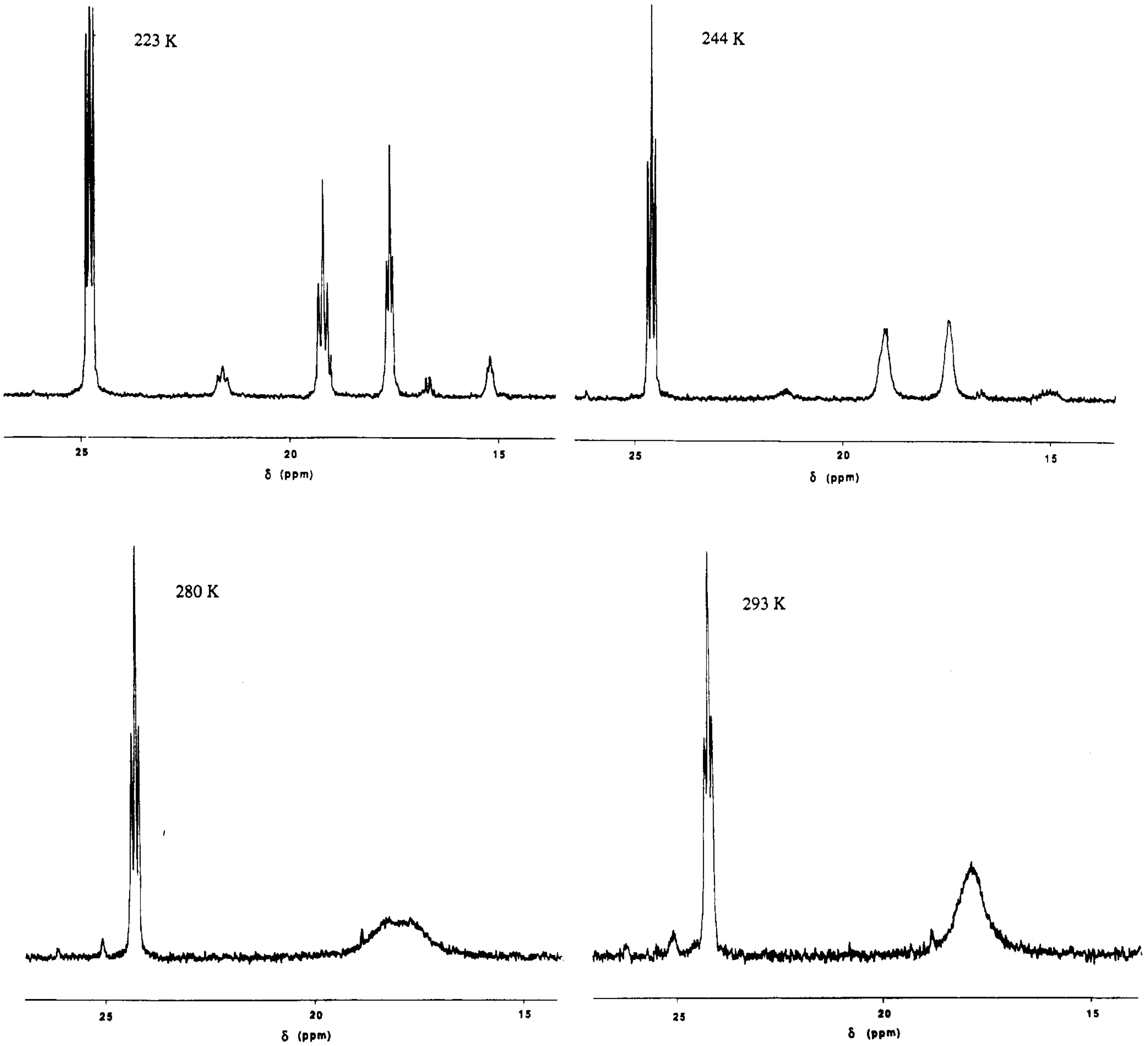

Figure 6. Variable temperature ^{31}P NMR spectra for *trans*-[PdCl$(PEt_3)_2(Ph_4P_2N_4S_2Me)$], **5**, in toluene-$d_8$.

sulfur bond, and the second invokes simultaneous inversions at the two sulfur atoms of the $P_2N_4S_2$ ring.

In order to determine the thermodynamic parameters for this fluxional process, the rate constants, k_r, have been determined at a series of temperatures for **4a–c** and **5** by computer line-shape fitting of the variable-temperature ^{31}P NMR spectra using the DNMR program of Kleier and Binsch.[34] The energies of activation for the dynamic exchange of phosphorus nuclei, E_a, were obtained from the slope of an Arrhenius plot [$\ln(k_r)$ vs $1/T$] while an Eyring plot [$\ln(k_r/T)$ vs $1/T$] enabled $\Delta H^{\circ *}$ and $\Delta S^{\circ *}$ to be calculated. Finally, $\Delta G^{\circ *}$ values were determined from the Gibbs equation. The thermodynamic parameters of activation for phosphorus exchange in **4a–c** and **5** are summarized in Table 6. The values of E_A fall within the narrow range 41–46 kJ mol^{-1} for all four complexes. On the basis of this low value of E_A we propose that the fluxional process involves rotation about the M–S bond rather than inversion at sulfur. This conclusion is consistent with the observation that E_A is independent of the nature of the organic group attached to S in **4a–c**. Furthermore, the activation energy is independent of the metal (**4a** vs **5**) indicating similar M–S bonding. We have been unable to locate any reports of analogous processes with which to compare these data.

Table 6. Thermodynamic Parameters (kJ mol^{-1}) for the Phosphorus Exchange in *trans*-[MCl$(PEt_3)_2(Ph_4N_4S_2R)$]

compound	E_a	$\Delta H^{\circ *}$	$\Delta G^{\circ *}$
trans-[PtCl$(PEt_3)_2\{\eta^1$-S-$Ph_4P_2N_4S_2Me\}$], **4a**	41	39	55
trans-[PtCl$(PEt_3)_2\{\eta^1$-S-$Ph_4P_2N_4S_2{}^tBu\}$], **4b**	41	39	54
trans-[PtCl$(PEt_3)_2\{\eta^1$-S-$Ph_4P_2N_4S_2Ph\}$], **4c**	46	44	54
trans-[PdCl$(PEt_3)_2\{\eta^1$-S-$Ph_4P_2N_4S_2Me\}$], **5**	44	42	52

Thermal Decomposition of PtCl$(PPh_3)_2(Ph_4P_2N_4S_2Me)$. In an attempt to prepare complexes of the type **4** with more bulky PR_3 ligands, the reaction of Li[$Ph_4P_2N_4S_2Me$] with *cis*-$PtCl_2(PPh_3)_2$ was investigated. Because of the very low solubility of the platinum reagent in THF at 23 °C, the reaction mixture was heated at 65 °C. Rather than the expected product *trans*-PtCl$(PPh_3)_2(\eta^1$-$Ph_4P_2N_4S_2Me$-*S*), a mixture of Pt$(PPh_3)_2(\eta^2$-$Ph_4P_2N_4S_2$-*S,S′*),[6] **6** (*ca.* 40%), and Pt$(PPh_3)(\eta^1$-THF-*O*)$(\eta^2$-$Ph_4P_2N_4S_2$-*S,S′*), (*ca.* 60%) was produced as determined by ^{31}P NMR spectroscopy. It seems likely that these products result from the process illustrated in Scheme 2 in which the expected η^1-S-bonded complex undergoes facile elimination of CH_3Cl to give the η^2-S,S′-bonded complex **6** followed by displacement of

---

[34] Kleier, D. A.; Binsch, G. Quantum Chemistry Program Exchange, Program No. 165. University of Indiana, Bloomingtonk, Indiana, 1969.

Scheme 2. Reaction of Li[$Ph_4P_2N_4S_2Me$] with *cis*-$PtCl_2(PPh_3)_2$ in THF at 65 °C

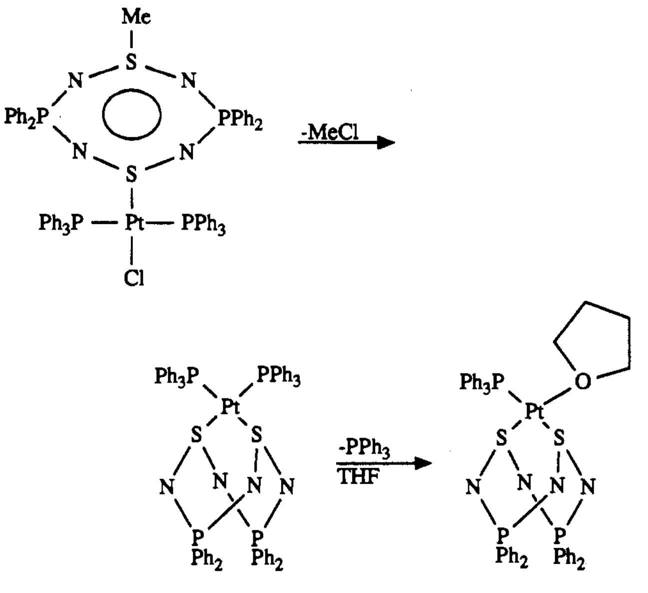

6

one PPh_3 ligand by THF. It has previously been established that **6** undergoes dissociation of PPh_3 upon mild heating to give a dimeric complex.[6] However, the possibility that the displacement of PPh_3 by THF occurs prior to the elimination of chloromethane cannot be ruled out.

Conclusions

The reaction of 1,1,5,5-tetraphenyldiphosphadithiatetrazocine (**1a**) with organolithium reagents occurs readily to give derivatives of the type Li[$Ph_4P_2N_4S_2R$] in which the eight-membered $P_2N_4S_2$ ring is retained and the organic group is attached to sulfur. In the solid state these organolithium derivatives form dimeric, step-shaped structures in which the two phosphorus atoms of each $P_2N_4S_2$ ring are inequivalent. ^{31}P and ^{7}Li NMR investigations reveal a fluxional process for the unsymmetrical dimers and provide evidence for a second, symmetrical, species in solution. The reaction of Li[$Ph_4P_2N_4S_2R$] with *cis*- or *trans*-$MCl_2(PEt_3)_2$ (M = Pt, Pd) produces complexes in which the metal is attached to the sulfur atom of the $Ph_4P_2N_4S_2R^-$ anion on the opposite side of the ring to the SR group. By contrast, early transition metals bind to this anion in an η^2-N,S fashion in complexes of the type $MCp_2Cl(Ph_4P_2N_4S_2R)$ (M = Ti, Zr, Hf).[35] Thus it appears that anions of the type $Ph_4P_2N_4S_2R^-$ will readily adapt their modes of ligation to accommodate the electronic requirements of individual metal centers. Studies aimed at defining the scope of the coordination chemistry of these novel anions are in progress.

Acknowledgment. We thank the NSERC (Canada) for financial support and Professor K. R. Dixon and Dr. D. E. Berry (University of Victoria, Canada) for many helpful discussions and assistance with the NMR simulation programs.

Supplementary Material Available: Tables of crystallographic data, hydrogen atom coordinates, anisotropic thermal parameters, bond lengths, bond angles, and torsion angles for (**3c**·THF)$_2$, rate plot data, thermodynamic parameters, and kinetics data and figures showing Eyring and Arrhenius plots for the phosphorus interchange in **4a–c** and **5** (24 pages).

---

(35) Chivers, T.; Hilts, R. W.; Parvez, M. *Inorg. Chem.*, in press.